Experimental Spectrum Sensor Testbed for Constructing Indoor Radio Environmental Maps

Elena Meshkova*, Junaid Ansari*, Daniel Denkovski†, Janne Riihijärvi*,
Jad Nasreddine*, Mihajlo Pavloski†, Liljana Gavrilovska† and Petri Mähönen*
* Institute for Networked Systems, RWTH Aachen University, Germany
† Faculty of Electrical Engineering and Information Technologies,
Ss. Cyril and Methodius University, Skopje, Macedonia
email: eme@inets.rwth-aachen.de

***Abstract*—In this paper we describe an experimental testbed to empirically study the construction of Radio Environmental Maps (REMs) in indoor environments. The testbed allows investigating the characteristics and modeling of the radio environment for indoor scenarios. The deployed system is a network of over 80 heterogeneous wireless spectrum sensors with significantly different measurement capabilities in an office building consisting of multiple rooms. As application examples we consider two scenarios, one illustrating the indoor propagation conditions and another showing temporal aspects of primary node activities as observed by sensing devices. The observed phenomena strongly indicate that development of general radio environment map solutions for indoor use are extremely challenging, unless heterogeneity of spectrum sensors and non-linearity of propagation conditions is considered. Our measurement results advocate dynamic construction of REMs instead of static solutions. We strongly believe that the deployed testbed and obtained experimental data can further facilitate research in the area of REMs.**

I. Introduction

The complexity of Radio Resource Management (RRM) in the indoor environment is rapidly increasing due to the growing number of heterogeneous wireless nodes operating within the buildings. Adding to this the already complex nature of the radio environment, solutions based on human intervention and manual optimization are becoming obsolete and inefficient. The *dynamic characterization and management of the radio environment* [1], [2] are the main solutions proposed to the above mentioned problems. In this context, Radio Environment Maps (REM) paradigm has been suggested as a support for RRM tools by providing a set of information that characterizes the radio environment as accurate as possible [1]. Building REMs for indoor environments is a real challenge due to the complex characteristics of these environments in terms of propagation and interference models, and their dynamics [3]–[5]. Therefore, dynamic environmental characteristics based on real time measurements are possible candidates to facilitate the efficient functioning of REMs in the indoor environment [6], [7]. Our another motivation for this work is the existing experimental research studying the outdoor environment for Dynamic Spectrum Access (DSA) opportunities, which provided promising insights into the outdoor spatial and temporal characteristics of received power levels [8], [9].

In this paper we describe the design and deployment of the testbed that allows us studying the characterization and modeling of the radio indoor environment based on spectrum measurements from heterogeneous spectrum sensors. The testbed is deployed over the area of $240\,\mathrm{m}^2$ that spans several rooms with both non load-bearing (paper) and bearing (semi-concrete) walls, the testbed allows to realistically study the indoor propagation conditions as perceived by three types of sensor devices. These device types, namely USRP2 [10], WARP [11] and TelosB [12], display a wide range of sensing and processing capabilities and to some extent reflect the characteristics that can be expected from a realistic heterogeneous network deployment. The testbed allows investigating the effect from both controlled and real user mobility as (a) some of the signal sources can be deployed on top of a toy train, and (b) a part of the testbed operates in a laboratory that is regularly used by varying number of people. Therefore, the testbed fulfills the necessary requirements for heterogeneity in both environmental and the hardware aspects of spectrum sensors to facilitate the study of both spatial and temporal spectral aspects of indoor environment in the context of cognitive wireless research.

The rest of the paper is structured as follows: Section II describes our deployment setup. In Section III we discuss the measurement results illustrating spatial and temporal signal patterns that can be observed using the testbed. Section IV draws conclusion remarks and gives directions for future work.

II. Testbed Design and Deployment

We have carried out the testbed deployment in a typical office space to study the implications of device sensitivity, sampling rates, and the spatial dependencies on REMs in a representative indoor environment. As described in the introduction our testbed fulfils the major requirements enabling the experimental research of indoor radio environment maps. These are: the *diversity of the environment* (e.g. different structures of the walls, diverse furniture placements in the rooms) and the *space* covered by the testbed; *heterogeneity of spectrum sensors*; support for *different user activity and mobility* patterns; and operation over *multiple frequencies*, enough to accommodate several independent channels [13].

TABLE I
MEASURED SENSITIVITY RANGES AND EXECUTION TIMINGS FOR DIFFERENT TYPES OF SPECTRUM SENSORS.

Spectrum sensors	Calibrated linear measurement range		Onboard execution timings (without PC communication)		Timings for spectrum sensing with communication delay to the PC for different frequency bandwidths			
	Min	Max	Spectrum sampling	Channel switching	Interface	5 MHz	20-25 MHz	2.402 -2.482 GHz
WARP	-90 dBm	-20 dBm	1.4 μs (RSSI)	22 μs	Ethernet	–	30 μs (22 MHz)	132 μs
USRP2	-75 dBm	-25 dBm	50 ns (IQ)	200 μs	Ethernet	2.02 ms	0.53 ms (20 MHz)	5.23 ms
TelosB	-90 dBm	-10 dBm	70 μs (RSSI)	740 μs	UART	3.5 ms	9.1 ms (25 MHz)	25.9 ms

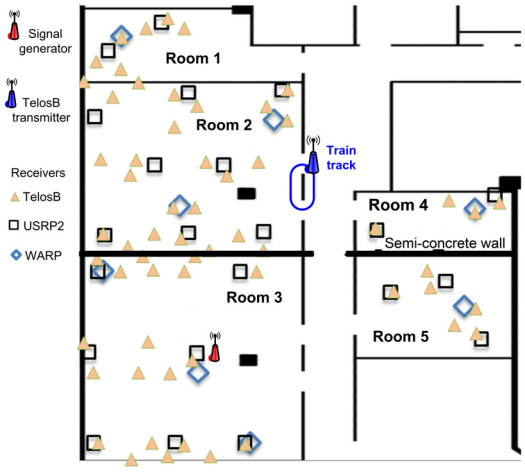

Fig. 1. The deployment map of different devices in an area of 12 m×20 m.

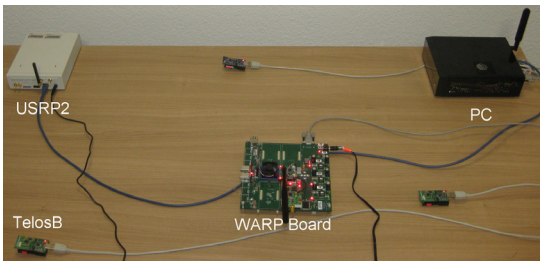

Fig. 2. Snapshot of a typical setup on an office table with a WARP board, a USRP2 board and three TelosB nodes attached to a PC. All the devices are uniquely accessible remotely via the LAN.

In our deployment setup, we have used 60 TelosB nodes, 20 USRP2 boards and 8 WARP boards. Fig. 1 shows the testbed deployment map in the office building consisting of five rooms. We have also deployed embedded PCs interfaced to these devices. The embedded PCs are part of the office LAN infrastructure so that the measurements can be controlled centrally through a remote machine. Furthermore, being part of the backbone, all the machines are synchronized using Network Time synchronization Protocol (NTP) [14]. Fig. 2 shows a typical deployment setup on an office table. We have developed spectrum sensing applications [15], [16] with flexible controlling APIs for all types of spectrum sensors and corresponding software scripts to enable efficient remote testbed control that includes conducting multiple repetitive experiments and gathering of the data in a systematic manner.

All the considered spectrum sensors operate in 2.4 GHz ISM band. Rice University's WARP SDR boards [11] and USRP2 boards from Ettus Research [10] have a sensing bandwidth of 22 MHz and 20 MHz respectively. Crossbow Inc. TelosB platforms [12] clocked at 4 MHz are transceivers with sensing bandwidth of 5 MHz. It should be noted that WARP and TelosB boards report the spectrum readings directly in terms of RSSI values, whereas USRP2 boards use two input channels for I and Q samples, which are then converted on the host PC into the power readings. Our spectrum sensing choice clearly falls into three distinct classes with different sensitivity levels and hardware capabilities. WARP board is a high end SDR platform providing extremely fast spectral data samples, USRP2 is a medium grade SDR platform, while TelosB represents a low-end device for spectrum sensing. Table I[1] summarizes the limits of sensing capabilities of all device types, which are dictated by their hardware capabilities and software applications that were developed for this testbed.

We have carefully profiled and then calibrated to the linear operating range the considered types of spectrum sensors by feeding a referenced signal from E4438C signal generator directly over a coaxial cable (see Table I). We have observed that the inconsistencies and biases among the devices of the same type are acceptably low. We also observed that USRP2 devices show strong non-linear behavior for low received powers, especially for levels below -75 dBm. Compared to the external monopole antennas for USRP2 and WARP boards, TelosB nodes have obviously slightly higher attenuation due to inverted F microstrip antenna.

As signal sources we used a programmable Agilent's E4438C signal generator and TelosB nodes. In this work for the continuous transmissions the E4438C generator was configured to produce QPSK modulated signal with 20 Msps and transmission power of 20 dBm. TelosB nodes were used to generate multi-source and moving signals, as well as periodic ON-OFF patterns following non-uniform distributions. These signals were produced using the test mode of CC2420 radio transceiver chip [17] on TelosB. The chip provides a continues 5 MHz wide signal with most of the power concentrated in a bandwidth of 2 MHz. The transmit power was set to 0 dBm.

III. EXAMPLES OF OBTAINED RESULTS

In this section we give illustrative examples of results that can be obtained using this testbed. We have considered two fundamental scenarios for this work. First we have studied the

[1]As most of the processing for USRP2 boards are happening to the host PC, its configuration influences the performance of the spectrum sensor. In our test we have used Core i7 based PC with Ubuntu x64 10.04 OS. The timing values for USRP2 are averaged over 10000 samples.

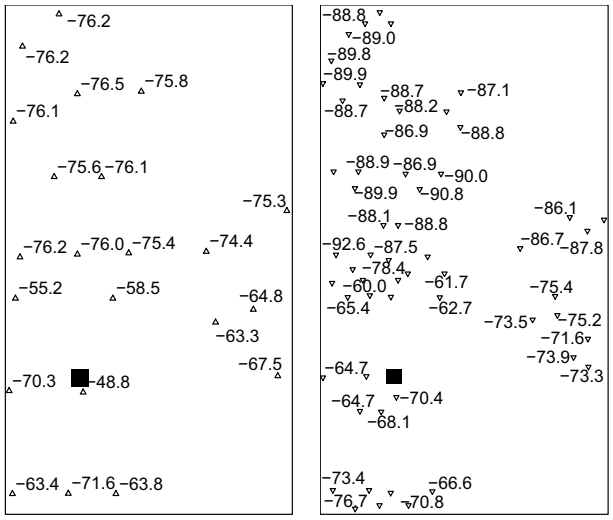

Fig. 3. Mean received power at the devices in dBm in an area of 12 m×20 m. Figure on the left shows data for USRP2 boards; the right figure displays data for TelosB nodes. The filled squares represent the position of the transmitter.

spatial aspects with a single transmitter sending a constant signal from the largest room (see Fig. 1). Then we have considered the implications of a moving transmitter. Finally, we have generated periodic ON-OFF signal patterns illustrating the *temporal* spectral aspects as observed by heterogeneous spectrum sensors[2].

A. *Influence of Propagation Environment*

Indoor propagation characteristics play one of the central roles in a number of application scenarios for REMs [18]. On the example of the constant signal transmitted by the E4438C signal generator we illustrate in Fig. 3 the overall distribution of received power readings as observed by different devices in the experimental indoor environment. The received power levels indicate a high variance in the measurements obtained by closely located sensors of the same, as well as of the different, types. This is due to the effect of propagation multipath, as one can observe non-linear and even non-monotonically decreasing function of the distance (cf. Fig. 4).

As an illustration we fit the data to the linear equation

$$P_i(\text{dBm}) = K - \alpha \log_{10}(d_i) - \beta C_i, \qquad (1)$$

where $P_i(\text{dBm})$ is the power received by node i, d_i is the distance between the sender and node i, and C_i is any further covariate value for node i to be used in the model. We have experimented with linear fitting (a) using only information on the distances d_i to the transmitter, and (b) adding C_i as the number of walls between the sender and the node i, as shown in Fig. 4. All walls are assumed to be homogenous with β corresponding to the drop in the received power per wall. We obtained the estimates $\hat{K}$, $\hat{\alpha}$ and $\hat{\beta}$ for the propagation model

[2]Before proceeding to the experiments, we studied the marginal densities of the results considering each type of sensors and the overall distribution of the received noise levels. We observed close-to-normal distributions of the received power for the noise, as sensed by different types of devices.

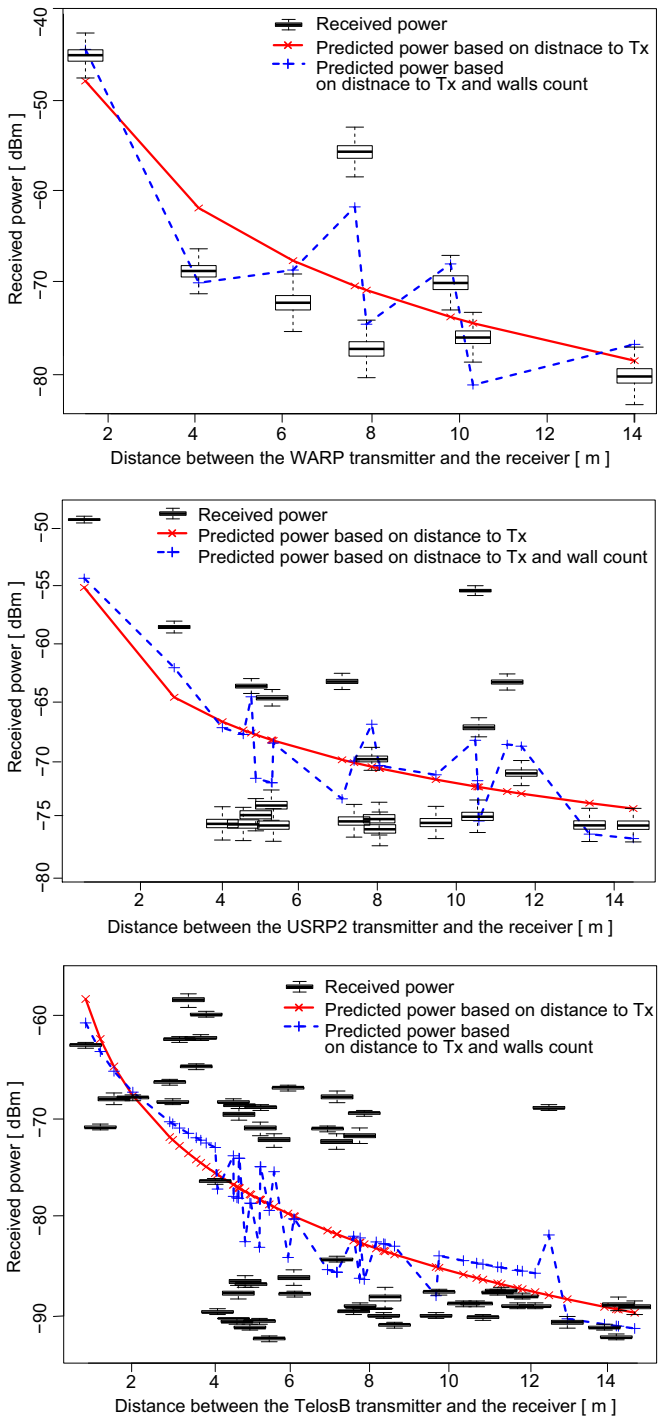

Fig. 4. Boxplots of the received power levels for the spectrum sensors at different distances to the transmitter, and results of linear fitting using the information on distances to the Tx and the walls. The figures show (from the top) the data for WARP boards, USRP2 devices and TelosB nodes.

parameters by simple least squares regression. For each fit we also studied the distribution of the residual estimation errors

$$P_i(\text{dBm}) - \hat{P}_i(\text{dBm}) = P_i(\text{dB}) - \hat{K} + \hat{\alpha} \log_{10}(d_i) + \hat{\beta} C_i \quad (2)$$

as well as their dependency on the distances d_i and the chosen covariates. Our experiments have shown that the linear fitting with information only on the locations of the receivers

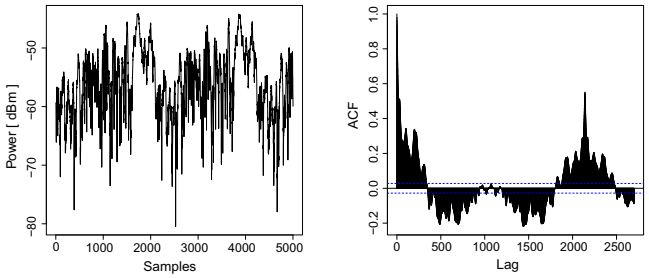

Fig. 5. Observed signals by the USPR2 board located near the moving transmitter. The left figure show the time series spectral data, whereas the right figure potrays the auto-correlation function (ACF) of the spectral data.

resulted in average estimation errors of 5.68 dB, 5.71 dB and 7.19 dB for WARPs, USRP2s and TelosB nodes respectively. The additional data on the number of walls between the transmitter and the receivers reduced the respective errors to 3.78 dB, 5.3 dB and 6.8 dB. These results indicate that, as expected, the classical propagation models do not fit well the indoor environment and more complex, maybe even non-linear models, have to be dynamically constructed or tuned to be applicable to the particular indoor conditions [5], [7].

B. Transmitter Mobility

The experiments with the mobile transmitter were carried out using a TelosB node as a signal source, which was placed on top of a model train moving with a constant speed of 5 m/s located as shown in Fig. 1. This resulted in a highly repetitive transmitter mobility patterns with short term variations caused in part by fast fading. While fast fading clearly severely affects the results, it is still possible to detect the underlying periodicity, at least given short correlation time for the channel as can be observed from Fig. 5.

C. ON-OFF Transmitter Patterns

In this scenario we illustrate the temporal structure of the power levels as observed by spectrum sensors. The basic characterizations of a duty cycled transmitter are the durations of the active (ON) and inactive (OFF) periods. The accurate estimation of the duty cycles, as well as ON-OFF activity periods can significantly enhance the channel sensing and selection processes for DSA networks [9], [19].

One may distinguish between several application scenarios for temporal spectrum sensing data:

1) estimation of ON and OFF power levels to determine if the channel is currently occupied;
2) estimation of several power levels, basically power-level clustering, is useful, for example to perform optimization of MAC-layer parameters or to try to identify multiple signal sources in the network;
3) prediction of the occupancy time for a particular frequency band.

Our testbed allows detecting signals with fairly high temporal resolution (see Table I) that is appropriate to record both packet-level and session-level behaviors in the packet-based

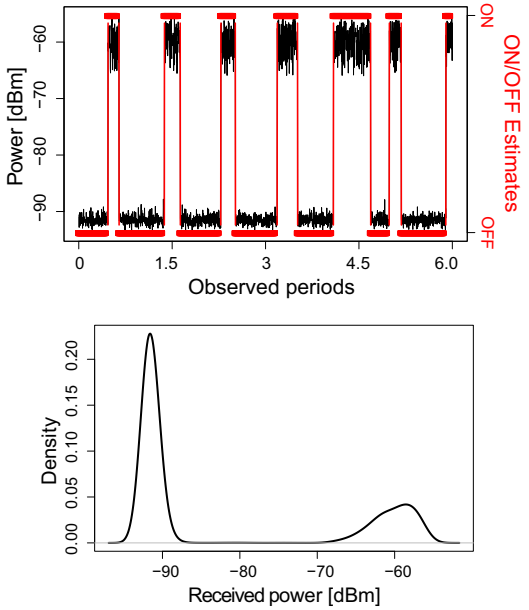

Fig. 6. The output of a WARP board receiving a strong signal, located at the distance of 0.5 meters from the transmitter. The top figure shows the received power levels and the estimated states ON-OFF activities of the transmitter. The lower figure portrays the estimated density of the received power levels.

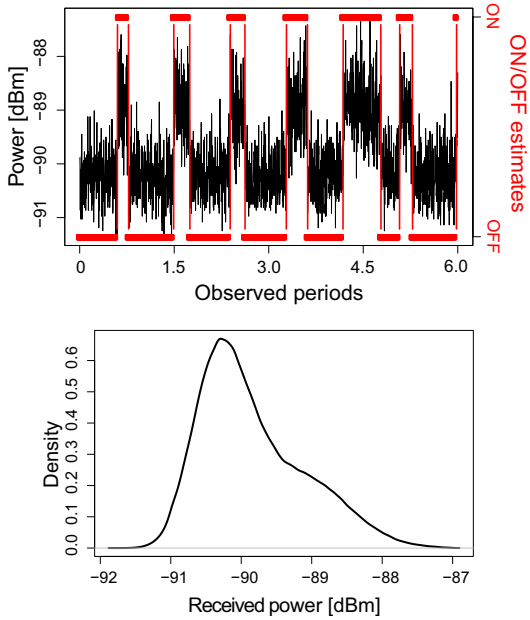

Fig. 7. The output of a WARP board receiving a weak signal, located at the distance of 11 m from the transmitter across the semi-concrete wall. The top figure shows the received power and the estimated ON-OFF states of the transmitter. The lower figure portrays the estimated density of the readings.

networks, for example IEEE 802.11g wireless networks. We have also programmed the TelosB nodes to generate energy levels with timings accurately following various ON-OFF distributions. These signals are useful to systematically study in practice the applicability of various sensing algorithms. The minimal duty cycle duration for these signals is 100 ms.

Fig. 6 shows ON-OFF activity patterns obtained from a single transmitter, which is a TelosB node generating a narrow-

band 5 MHz signal with ON-OFF periods following a gamma distribution. The duty cycle of the signal is 25%, with average ON period of 1.25 seconds and variance of 20%. The results are obtained from two WARP boards placed at different distances from the transmitter. As shown in Fig. 6 and 7 the density functions of the received power by these boards are significantly different and additional processing is needed to estimate the distributions of the received power corresponding to ON and OFF periods for the weak signal.

Depending on the application scenario mechanisms of different complexity have to be applied for data post-processing. For the first two scenarios for application of temporal data, when the environmental conditions are relatively stable and difference between power levels is significantly large, often very simple techniques can be used (a sample signal is shown in Fig. 6). For e.g., the local minima of the density functions of the data can serve as a thresholds for distinguishing between different power levels. For weaker signals we can use moving average to smooth the data beforehand. This will ease the data analysis at the cost of losing some of the data granularity.

However, if the propagation conditions are severe or we want to extract additional information from the data to enable the third application scenario, we require more complex processing. We have utilized the combination of Hidden Semi-Markov Models (HSMM) [20], [21] to determine the distribution of durations of ON and OFF periods that are used to predict the channel occupancy duration [22], as well as to distinguish between different power levels. These results can be used as a basis when studying MAC-layer sensing solutions for cognitive wireless networks. The learning of HSMM structure resulted in quite accurate estimations of the distributions of ON and OFF periods. For instance, we have observed up to %1 accuracy in estimation of the duty cycle. Furthermore, we have applied the estimated model as one of the prior inputs to the Viterbi algorithm [21], [23], which resulted in accurate classification of spectrum samples into the ON and OFF states, as shown in Fig. 6 and Fig. 7.

IV. Conclusions

In this paper we have presented the experimental testbed for studying the implications indoor environments pose to cognitive radio technologies relying on power spectrum sensing. We provided sample results related to both spatial and temporal aspects of this problem. Our data is obtained from a unique dataset generated by a 80+ node measurement network consisting of highly heterogeneous spectrum sensors. Based on this dataset, we showed the differences between the measurements carried out by various sensor types. We also observed the effects of fast-fading and mobility that can drastically affect the received power and lead to misinterpretation of the readings. In the spacial domain we recorded major variations in the data gathered by the nearby nodes. All of this strongly indicates that development of general radio environment map solutions for indoor use will be extremely challenging and, it is likely that the dynamic approach to constructing REMS has to be adopted. We believe that more measurement-driven theoretical and modeling work is required to understand the *network-wide* behavior of the indoor radio environment.

Acknowledgment

The authors thank the European Union for providing partial funding of this work through the ACROPOLIS and FARAMIR projects. We thank V. Atanasovski for fruitful discussions.

References

[1] Y. Zhao, B. Le, and J. H. Reed, *Cognitive Radio Technology*. Elsevier, 2006, ch. Network Support: The Radio Environment Map, pp. 337–363.

[2] I. F. Akyildiz, W.-Y. Lee, M. C. Vuran, and S. Mohanty, "Next generation/dynamic spectrum access/cognitive radio wireless networks: a survey," *Computer Networks*, vol. 50, no. 13, pp. 2127 – 2159, 2006.

[3] R. J. Bultitude, "Measurement, characterization and modeling of indoor 800/900 mhz radio channels for digital communications," *IEEE Communications Magazine*, vol. 25, no. 6, pp. 5 – 12, jun 1987.

[4] H. Hashemi and *et. al*, "Measurements and modeling of temporal variations of the indoor radio propagation channel," *IEEE Transactions on Vehicular Technology*, vol. 43, no. 3, pp. 733 –737, aug 1994.

[5] I. Kashiwagi, T. Taga, and T. Imai, "Time-varying path-shadowing model for indoor populated environments," *IEEE Transactions on Vehicular Technology*, vol. 59, no. 1, pp. 16 –28, jan. 2010.

[6] H. Hashemi, "The indoor radio propagation channel," *Proceedings of the IEEE*, vol. 81, no. 7, pp. 943 –968, July 1993.

[7] M. F. Hanif, P. J. Smith, and M. Shafi, "Performance of cognitive radio systems with imperfect radio environment map information," in *Australian Communications Theory Workshop*, Feb. 2009, pp. 61 –66.

[8] M. Wellens, J. Wu, and P. Mähönen, "Evaluation of spectrum occupancy in indoor and outdoor scenario in the context of cognitive radio," in *Proc. of CROWNCOM*, August 2007.

[9] M. Wellens, J. Riihijärvi, and P. Mähönen, "Evaluation of Adaptive MAC-Layer Sensing in Realistic Spectrum Occupancy Scenarios," in *IEEE DySpan*, May 2010, pp. 1–12.

[10] "The USRP Board," https://radioware.nd.edu/documentation/hardware/the-usrp-board [Last visited: March 10, 2011].

[11] A. Khattab and *et. al*, "WARP: a flexible platform for clean-slate wireless medium access protocol design," *SIGMOBILE Mob. Comput. Commun. Rev.*, vol. 12, no. 1, pp. 56–58, 2008.

[12] *TelosB Node*, Crossbow Inc., http://www.willow.co.uk/TelosB_Datasheet.pdf, Last visited: 11.06.2010.

[13] K. Chowdhury and T. Melodia, "Platforms and testbeds for experimental evaluation of cognitive ad hoc networks," *Communications Magazine, IEEE*, vol. 48, no. 9, pp. 96–104, 2010.

[14] D. Mills, "Internet time synchronization: The network time protocol," *IEEE Trans. on Communications*, vol. 39, no. 10, pp. 1482–1493, 2002.

[15] D. Denkovski, V. Atanasovski, and L. Gavrilovska, "Efficient mid-end spectrum sensing implementation for cognitive radio applications based on usrp2 devices," in *in Proc. of COCORA*, April 2011.

[16] J. Ansari, T. Ang, and P. Mähönen, "WiSpot - detecting Wi-Fi networks using IEEE 802.15.4 radios," in *EWSN*, Feb. 2011.

[17] "Chipcon CC2420 datasheet," Last visited: 15.06.2010, http://www.chipcon.com/files/CC2420_Data_Sheet_1_3.pdf.

[18] H. Celebi, I. Guvenc, S. Gezici, and H. Arslan, "Cognitive-Radio Systems for Spectrum, Location, and Environmental Awareness," *Antennas and Propagation Magazine, IEEE*, vol. 52, no. 4, pp. 41–61, 2010.

[19] S. Geirhofer, L. Tong, and B. Sadler, "Dynamic spectrum access in the time domain: Modeling and exploiting white space," *IEEE Communications Magazine*, vol. 45, no. 5, p. 66, 2007.

[20] Y. Guédon, "Estimating hidden semi-Markov chains from discrete sequences," *Journal of Computational and Graphical Statistics*, vol. 12, no. 3, pp. 604–639, 2003.

[21] J. O'Connell and S. Højsgaard, *mhsmm: Parameter Estimation and Prediction for Hidden Markov and Semi-Markov models for Data with Multiple Observation Sequences*, R package v. 0.3.6, 2010, http://CRAN.R-project.org/package=mhsmm.

[22] H. Kim and K. Shin, "Efficient discovery of spectrum opportunities with MAC-layer sensing in cognitive radio networks," *IEEE Transactions on Mobile Computing*, pp. 533–545, 2007.

[23] A. Viterbi, "Error bounds for convolutional codes and an asymptotically optimum decoding algorithm," *IEEE Transactions on Information Theory*, vol. 13, no. 2, pp. 260–269, 2002.